Measurement of the Neutron Spin Asymmetry in the Deep Valence Quark Region at Jefferson Lab 12 GeV

Xiaochao Zheng,[a,*] **Mingyu Chen**[a] **and Carter Hedinger**[a] **on behalf of the Jefferson Lab E12-06-110 Collaboration**

[a]*University of Virginia,*
  382 McCormick Rd., Charlottesville, VA 22904, USA

  E-mail: xz5y@virginia.edu, mc4ne@Virginia.edu, ch9bx@virginia.edu

After decades of study of the nucleon spin structure, the deep-valence quark (high x) region remains difficult to access experimentally. On the other hand, the high-x region is a clean testing ground of various predictions for the ratio of polarized and unpolarized structure functions, and quark polarization inside the nucleon. These predictions include relativistic constituent-quark model, perturbative QCD, holographic light-cone QCD, and Schwinger-Dyson equations. We report on a 12 GeV Jefferson Lab experiment (JLab E12-06-110) that measured the virtual photon asymmetry of the neutron, A_1^n. The experiment used a longitudinally polarized beam of 10.4 GeV energy and a polarized ^{3}He target in Hall C. It pushed the highest x value from $x = 0.61$ of the 6 GeV era to $x = 0.75$. Preliminary results and the current status of the analysis are presented.

---

*Speaker

1. Introduction

The spin structure of the nucleon provides important information on our understanding of the strong interaction and a testing ground on its theory, quantum chromodynamics (QCD). Since the "proton spin crisis" in the 1980's [1], significant knowledge has been accumulated on how the spin of the proton emerges from its fundamental quark and gluon constituents. The Jaffe-Manohar spin sum rule [2] states that the nucleon spin can be decomposed into four components: the valence and sea quark intrinsic spin $\Delta\Sigma$, quark orbital angular momentum (OAM) L_q, gluon intrinsic spin ΔG, and gluon OAM L_g:

$$\frac{1}{2} = \frac{1}{2}\Delta\Sigma + \Delta G + L_q + L_g \ . \tag{1}$$

Furthermore, the Ji sum rule [3] provides a gauge-invariant decomposition of the nucleon spin into quark helicity, quark orbital, and the gluon contribution J_g:

$$\frac{1}{2} = \frac{1}{2}\Delta\Sigma + L_q + J_g \ . \tag{2}$$

Existing world data show that the quark spin $\Delta\Sigma$ contributes to about 30% of the proton spin [4], with the rest coming from quark OAM and gluons.

A large experimental program focusing on understanding the proton spin structure is ongoing or being planned, to pin down precisely these components and their dependence on other parameters of the quark dynamics such as the Bjorken scaling variable x. For recent reviews, see [5, 6]. In the deep inelastic scattering (DIS) regime, x represents the fraction of the longitudinal momentum of the nucleon (or hadron) that is carried by a specific quark or gluon. The probability to find the quark at a specific value of x is described by its parton distribution function (PDF), with its polarization described by the polarized PDF.

One useful observable in the nucleon spin structure study is the virtual photon asymmetry A_1, defined as

$$A_1(x, Q^2) \quad \equiv \quad \frac{\sigma_{1/2} - \sigma_{3/2}}{\sigma_{1/2} + \sigma_{3/2}} = \frac{g_1(x, Q^2) - \gamma^2 g_2(x, Q^2)}{F_1(x, Q^2)} \ . \tag{3}$$

where the subscripts $1/2, 3/2$ represents the total spin of the photon-nucleon system. The asymmetry A_1 can be related to the unpolarized and polarized structure functions F_1 and $g_{1,2}$ as shown above, where $\gamma^2 \equiv \frac{(2Mx)^2}{Q^2}$ with M the nucleon mass and Q^2 the negative of the four-momentum transfer squared of the DIS process. In practice, data are taken with the target spin direction aligned both parallel and perpendicular to the beam direction to provide the "electron asymmetry" $A_\parallel$ and $A_\perp$, which can be combined to form A_1 through kinematic factors.

The value of A_1 becomes particularly interesting in the so-called large x region of DIS, typically $0.5 < x < 1.0$. The closer x is to 1, the more energy of the nucleon is carried by the quark struck by the virtual photon and less by the spectator quarks. Furthermore, less energy can be spared to generate quark-antiquark sea and the scattering can be viewed as primarily from a valence constituent quark.

Under the condition that quarks are quasi-free point-like particles, and in the absence of orbital motion, the initial state with total spin $1/2$ would dominate Eq. (3) because only in this state could

the quark absorb the spin of the virtual photon, producing a spin flip of the quark itself. In this case, $A_1 \to 1$ as $x \to 1$. On the other hand, models that account for the interaction between the struck and spectator quarks, particularly non-perturbative treatment such as Dyson-Schwinger Equation), could imply $A_1 < 1$ and differ between the proton and the neutron because of their different quark flavor contents. Predictions for A_1 as well as other structure function ratios are shown in Table 1. Notable is the polarization of the quarks, $\Delta u/u$ and $\Delta d/d$, which can be extracted from experiments by combining proton with neutron data. Most predictions for $\Delta d/d$ are negative, while perturbative QCD (pQCD) and holographic light-front QCD (HLFQCD) [7] provide the prediction $\Delta d/d \to 1$. The latest JLab 6 GeV high x data showed that $\Delta d/d$ remains negative up to $x = 0.61$ [8, 9], which triggered significant interest and the hypothesis that the down quarks possess sizable orbital motion [10]. Nevertheless, when $x = 1$, orbital motion diminishes and more recent theoretical work predicted that $\Delta d/d$ turns positive at higher x values than covered by the data [7, 10].

Model	$\frac{F_2^n}{F_2^p}$	$\frac{d}{u}$	$\frac{\Delta d}{\Delta u}$	$\frac{\Delta u}{u}$	$\frac{\Delta d}{d}$	A_1^n	A_1^p
DSE-1	0.49	0.28	-0.11	0.65	-0.26	0.17	0.59
DSE-2	0.41	0.18	-0.07	0.88	-0.33	0.34	0.88
$0_{[ud]}^+$	$\frac{1}{4}$	0	0	1	0	1	1
NJL	0.43	0.2	-0.06	0.8	-0.25	0.35	0.77
SU(6)	$\frac{2}{3}$	$\frac{1}{2}$	$-\frac{1}{4}$	$\frac{2}{3}$	$-\frac{1}{3}$	0	$\frac{5}{9}$
CQM	$\frac{1}{4}$	0	0	1	$-\frac{1}{3}$	1	1
pQCD	$\frac{3}{7}$	$\frac{1}{5}$	$\frac{1}{5}$	1	1	1	1
HLFQCD	0.28	0.035	0.035	1	1	1	1

Table 1: Predictions for $x = 1$ value of various models [7, 11, 12].

2. Jefferson Lab Experiment E12-06-110

The primary goal of the JLab 12 GeV experiment E12-06-110 [13] is to measure the neutron spin asymmetry A_1^n in the deep valence quark region, up to $x = 0.75$. The experiment was carried out in experimental Hall C, using a longitudinally polarized electron beam of energy 10.4 GeV at 30 μA and a 40-cm long polarized ^{3}He target. The target system was installed and commissioned between November 2019 and January 2020. Production data were taken between January 12 and March 13, 2020. Two glass cells, named Dutch and BigBrother, were used. Another experiment E12-06-121 [14], carried out after E12-06-110, utilized the same polarized ^{3}He target and measured d_2^n, a moment of the neutron spin structure functions.

To access the neutron spin asymmetry A_1^n, inclusive scattering data were collected using the two Hall C spectrometers, namely the High Momentum Spectrometer (HMS) and the Super High Momentum Spectrometer (SHMS). Both spectrometers were positioned at 30° from the beamline for DIS data taking, see Table 2 for the spectrometer central momentum setting and the target cell used. For each setting, data were taken on both $A_\parallel$ and $A_\perp$. The majority of the production beam time was spent on $A_\parallel$ at the higher E_p settings. A small amount of beam time was also taken for $e-{}^3$He elastic and $\Delta(1232)$ production using a 2.13 GeV beam to determine the absolute sign of the

measured parallel and transverse asymmetries, respectively. For these calibration runs, the SHMS was positioned at $8.5°$ and the HMS at $11.5°$.

Kine	Spec	E_b	E_p	θ	Cell
3	HMS	10.38	2.9	30°	Bigbrother
4	HMS	10.38	3.5	30°	Dutch& Bigbrother
B	SHMS	10.38	2.6	30°	Dutch& Bigbrother
C	SHMS	10.38	3.4	30°	Bigbrother

Table 2: Beam energy and spectrometer settings (central momentum E_p and angle θ) for DIS production runs of E12-06-110.

2.1 The Polarized ^{3}He Target

As mentioned earlier, a polarized ^{3}He target was used for the experiment, which acts as an effective polarized neutron target. The target was polarized using the spin-exchange optical pumping (SEOP). As part of a long history of using SEOP polarized ^{3}He target to study the spin structure of the nucleon that traces back to SLAC E142/154 and JLab 6 GeV program, this experiment utilized a new technique where the gas exchange between the (top) pumping chamber and the (bottom) target chamber is facilitated by thermal convection, see Fig. 1 left. The in-beam target polarization reached about 55% with a 30 μA beam, a near factor two increase on the figure-of-merit (FOM), defined by the beam current and the target polarization as $I_{\text{beam}}P_{\text{targ}}^2$, see Fig. 1 right. The detailed run-to-run target polarization is given in Fig. 2.
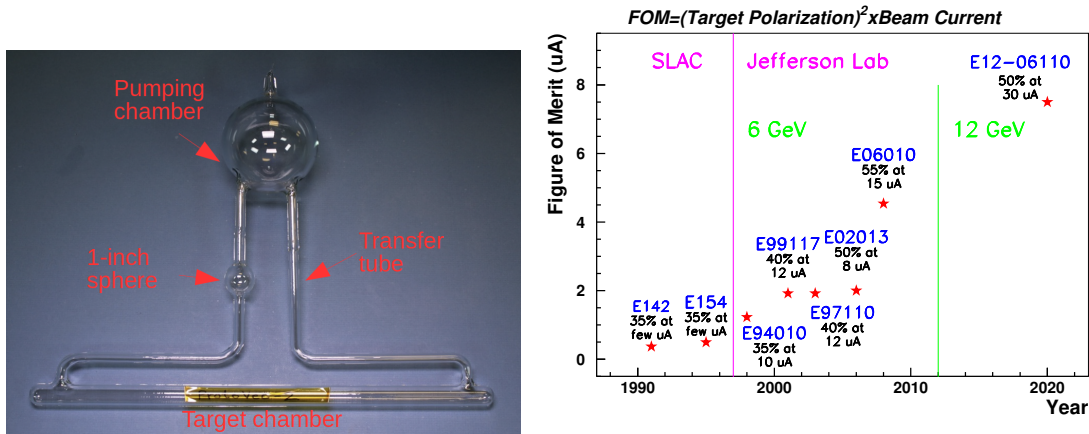

Figure 1: Left: the so-called "convection design" of polarized ^{3}He target cell used by the 12 GeV era JLab experiments. One of the transfer tubes was heated to induce thermal convection flow; Right: figure-of-merit of SEOP-based polarized ^{3}He targets from SLAC and JLab 6 GeV era to this experiment.

2.2 The Polarized Electron Beam

The polarized electrons are generated through the photoelectric effect with the driving laser circularly polarized. The average beam polarization during the experiment was determined from
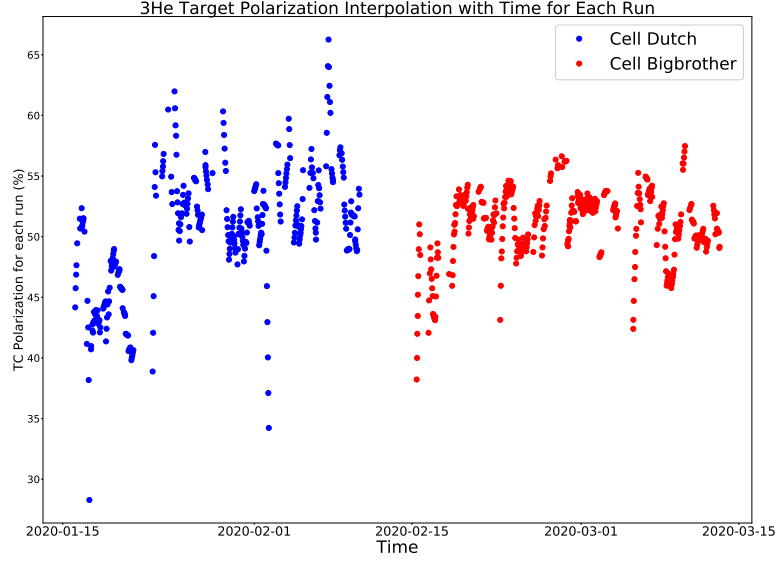
Figure 2: Target polarization vs. time for the A_1^n experiment.

Moller polarimetry to be 85.4% with a ±0.3% statistical precision. The systematic uncertainty includes a ±1.8% contribution due to the polarimetry device and a ±0.8% contribution due to variation in the beam polarization. Work is being carried out to reduce the systematic uncertainty to ±0.9% by correcting with the measured beam energy on a run-to-run basis. The beam helicity followed a pseudo-random quartet sequence with the spin flip rate at 120 Hz. Due to the very low rate of large x DIS events, it was necessary to mix a 120-Hz pulser with DIS events to ensure accurate decoding of the helicity signal. The helicity-dependent variation in the beam charge was controlled by a real-time feedback at the source level.

2.3 Data analysis

The data analysis, carried out primarily in two PhD thesis work [15, 16], followed a similar procedure as the previous 6 GeV A_1^n experiment [17]. Starting from the inclusively scattered particle detected by each spectrometer, a series of event selection "cuts" were applied. These included spectrometer acceptance cuts, particle identification cuts utilizing signals detected by the gas cherenkov detector and the electromagnetic calorimeter, and beam trip cuts to select events that were collected at the nominal beam current of 30μA.

The raw asymmetry was formed using event counts $N^\pm$ collected in the beam helicity + and - windows:

$$A_{\text{raw}} = \pm \frac{\dfrac{N^+}{Q^+\eta_{LT}^+} - \dfrac{N^-}{Q^-\eta_{LT}^-}}{\dfrac{N^+}{Q^+\eta_{LT}^+} - \dfrac{N^-}{Q^-\eta_{LT}^-}},$$

where $Q^\pm$ and $\eta_{LT}^\pm$ represent the beam charge and the DAQ livetime correction factor, respectively. The overall sign (+ or − on the RHS) was determined by the elastic longitudinal and $\Delta(1232)$

transverse asymmetries [15]. The raw asymmetry was then corrected for the beam and target polarizations, and dilution of unpolarized events from the target glass windows and the N_2 mixed with the ^{3}He gas:

$$A_{\parallel,\perp} = \frac{A_{\text{raw}}}{P_b P_t f_{N_2} f_{\text{window}}}.$$

The N_2 in the ^{3}He target is unpolarized but necessary to enable SEOP. The N_2 dilution was evaluated using data taken with a reference glass cell filled with N_2 gas, combined with a simulation that accounted for the different radiative effects between production cells and the reference cell. Similarly, the dilution from the up- and down-stream glass windows of the polarized ^{3}He cell was evaluated using data taken with an empty reference glass cell combined with simulation. For the final analysis, a cut on the vertex $z = (-15, 15)$ cm was used which eliminated events from the glass windows.

In addition, the data analysis of this experiment included two careful steps: First, it was observed that some of the data were taken with the electron beam slightly off-center from the target glass cell, resulting in beam "scraping" off the glass walls. It was found that this effect can be sufficiently suppressed using the PID cuts [15]. Second, the asymmetry was extracted with varying size of the spectrometer angle acceptance and a fluctuation beyond what is typically expected from statistical effects was observed with the widest cuts. As a result, a set of moderate angle acceptance cuts was used, yielding slightly lower statistics [16].

3. Preliminary Results on ^{3}He Asymmetries

Once the electron asymmetries $A_{\parallel,\perp}$ were extracted, they were combined to form A_1 of ^{3}He. The data were binned in E_p, which were then converted to x. Binning data in E_p will allow additional corrections to be made to the ^{3}He asymmetries, see next section. The asymmetry $A_1(^3\text{He})$ with DIS cut $W > 2$ GeV where W is the invariant mass of the photon-nucleon system, is shown in Fig. 3 and those without the DIS cut in Fig. 4. Similar results were also formed for the asymmetry A_2 and the structure function ratios g_1/F_1 and g_2/F_2, all on ^{3}He. Generally speaking, the new results agree very well with past data from the JLab 6 GeV era, though they do exhibit a milder x dependence. Note that radiative corrections still need to be applied to these asymmetry results.

4. Future Work

The radiative correction can be done using either data or world parameterization of the structure functions as inputs. For typical DIS, the true vertex kinematic variables correspond to an incoming electron of energy lower than that of the electron beam, $E < E_b$, and the outgoing electron of energy higher than that of the spectrometer momentum acceptance, $E' > E_p$. In data-driven radiative corrections, one must have sufficient data in this (E, E') region. In Fig. 5, we show all existing polarized ^{3}He data from JLab. The (E_b, E_p) setting of this experiment is given as purple vertical lines (while that of the d_2^n experiment shown in green). One can see that all previous data were collected with a beam energy below 6 GeV and thus populate a small portion of the (E, E') range needed by radiative correction of this experiment. Therefore, we plan to use a
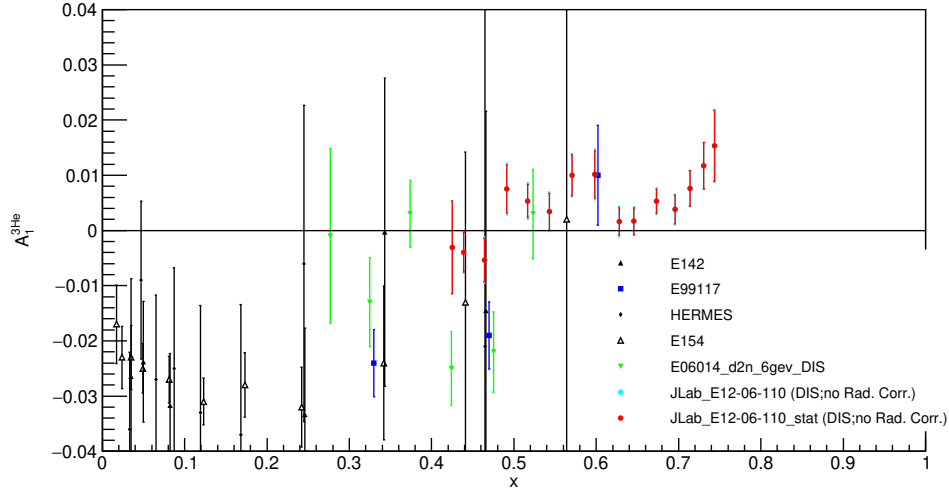
Figure 3: Results of $A_1^{^3\mathrm{He}}$ (red solid circles) as a function of the Bjorken x with the DIS cut $W > 2$ GeV. Radiative corrections have not been applied yet. The error bars included both statistical uncertainty (red), and the total uncertainty (cyan), though the latter is barely visible.
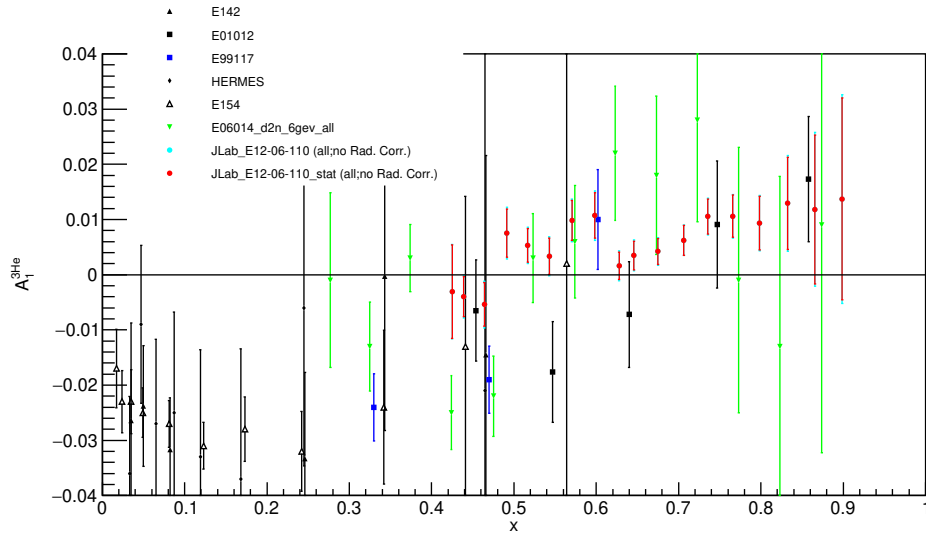

Figure 4: Results of $A_1^{^3He}$ (red solid circle) as a function of Bjorken x with no DIS cut applied. Radiative corrections have not been applied yet. The error bars included both statistical uncertainty (red), and the total uncertainty (cyan), though the latter is barely visible.

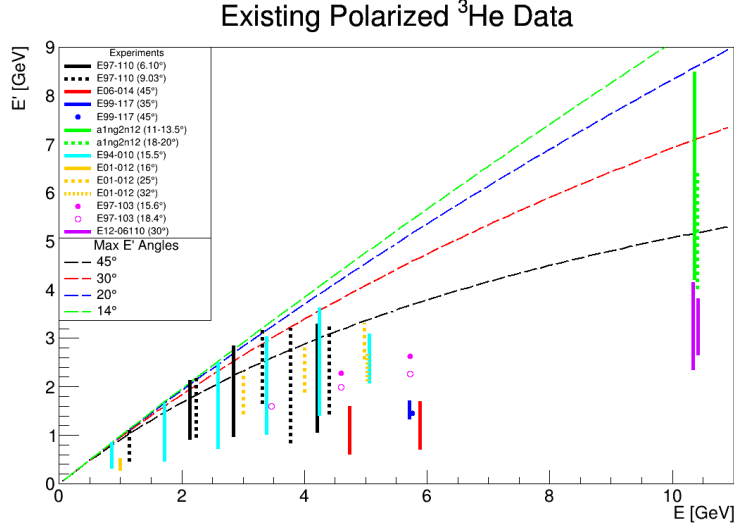parameterization as input to the radiative corrections, supplemented by a cross check with existing data.

Figure 5: Kinematic coverage of all existing polarized ^{3}He experiments carried out at JLab [5]. The A_1^n (green vertical line) and d_2^n (purple vertical line) experiments are shown on the far right. To perform radiative corrections, we need input data or model to cover the full region enclosed by elastic scattering (dashed colored curves), the experimental setting itself (vertical line on the far right), and a horizontal line (not drawn) that forms a (nearly) triangular shape.

After radiative corrections are applied to ^{3}He asymmetries, the next step is to obtain neutron asymmetries and structure function ratios. This is referred to as "nuclear correction" which removes nuclear effects that arise from nuclear binding, shadowing, anti-shadowing, potential spin depolarization, Fermi motion, off-shell, and non-nucleonic degrees of freedom. In previous experiments, A_1^n was extracted from $A_1^{^3He}$ as:

$$A_1^n = \frac{1}{\tilde{P}_n} \frac{F_2^{^3He}}{F_2^n} \left(A_1^{^3He} - \tilde{P}_p \frac{F_2^p}{F_2^{^3He}} A_1^p \right), \tag{4}$$

where $P_p = -0.028^{+0.009}_{-0.004}$ and $P_n = 0.086^{+0.036}_{-0.02}$ are the effective nucleon polarization of the neutron and proton inside ^{3}He, while $\tilde{P}_p = P_p - 0.014$ and $\tilde{P}_n = P_n + 0.056$ account for additional effects from pre-existing $\Delta(1232)$ states. Structure function ratios A_2, g_1^n/F_1^n, and g_2^n/F_2^n can be extracted from ^{3}He quantities in a similar manner.

Once the neutron spin structure functions are extracted, they can be combined with data on the proton to further study the quark polarizations. This allows for the separation of the ratios of polarized to unpolarized PDFs for up and down quarks:

$$\frac{\Delta u + \Delta \bar{u}}{u + \bar{u}} = \frac{4}{15} \frac{g_1^p}{F_1^p} (4 + R^{du}) - \frac{1}{15} \frac{g_1^n}{F_1^n} (1 + 4R^{du}) \tag{5}$$

$$\frac{\Delta d + \Delta \bar{d}}{d + \bar{d}} = -\frac{1}{15} \frac{g_1^p}{F_1^p} (1 + \frac{4}{R^{du}}) + \frac{4}{15} \frac{g_1^n}{F_1^n} (4 + \frac{1}{R^{du}}), \tag{6}$$

where the ratio $R^{du} = \frac{d+\bar{d}}{u+\bar{u}}$ can be obtained from world parameterizations. For A_1^P and g_1^P/F_1^P, we can either use second-order polynomial fits to the world data [18], or use results from the JLab CLAS12 Run Group C (RGC) experiment [19].

5. Conclusion and Outlook

We report here status of the recently completed JLab 12 GeV experiment E12-06-110. Data were collected for DIS using a polarized ^{3}He target up to $x = 0.75$, beyond the previous 6 GeV experiment (which reached $x = 0.61$). Preliminary results on the ^{3}He asymmetry A_1, absent of radiative corrections, are in good agreement with existing data, though they appear to have a milder x dependence. Work still needs to be done on the radiative corrections and extraction of the neutron information and the quark polarizations. It would be interesting to study also the impact a possible energy upgrade of JLab can bring to this topic, which is presented in another proceeding contribution to this Symposium [20].

Acknowledgments

References

[1] European Muon collaboration, J. Ashman et al., *A Measurement of the Spin Asymmetry and Determination of the Structure Function g(1) in Deep Inelastic Muon-Proton Scattering*, *Phys. Lett. B* **206** (1988) 364.

[2] R. L. Jaffe and A. Manohar, *The G(1) Problem: Fact and Fantasy on the Spin of the Proton*, *Nucl. Phys. B* **337** (1990) 509–546.

[3] X. Ji, *Gauge-invariant decomposition of nucleon spin*, *Phys. Rev. Lett.* **78** (Jan, 1997) 610–613.

[4] S. E. Kuhn, J. P. Chen and E. Leader, *Spin Structure of the Nucleon - Status and Recent Results*, *Prog. Part. Nucl. Phys.* **63** (2009) 1–50, [0812.3535].

[5] A. Deur, S. J. Brodsky and G. F. De Téramond, *The Spin Structure of the Nucleon*, 1807.05250.

[6] X. Ji, F. Yuan and Y. Zhao, *What we know and what we don't know about the proton spin after 30 years*, *Nature Rev. Phys.* **3** (2021) 27–38, [2009.01291].

[7] T. Liu, R. S. Sufian, G. F. de Téramond, H. G. Dosch, S. J. Brodsky and A. Deur, *Unified Description of Polarized and Unpolarized Quark Distributions in the Proton*, *Phys. Rev. Lett.* **124** (2020) 082003, [1909.13818].

[8] JEFFERSON LAB HALL A collaboration, X. Zheng et al., *Precision measurement of the neutron spin asymmetry A_1^n and spin flavor decomposition in the valence quark region*, *Phys. Rev. Lett.* **92** (2004) 012004, [nucl-ex/0308011].

[9] JEFFERSON LAB HALL A collaboration, X. Zheng et al., *Precision measurement of the neutron spin asymmetries and spin-dependent structure functions in the valence quark region*, *Phys. Rev. C* **70** (2004) 065207, [nucl-ex/0405006].

[10] H. Avakian, S. J. Brodsky, A. Deur and F. Yuan, *Effect of Orbital Angular Momentum on Valence-Quark Helicity Distributions*, *Phys. Rev. Lett.* **99** (2007) 082001, [0705.1553].

[11] C. D. Roberts, R. J. Holt and S. M. Schmidt, *Nucleon spin structure at very high-x*, *Phys. Lett. B* **727** (2013) 249–254, [1308.1236].

[12] T. Liu. private communication, 2023.

[13] X. Zheng (contact), G. Cates, J. Chen, Z.-E. Meziani et al., "Measurement of Neutron Spin Asymmetry A_1^n in the Valence Quark Region Using an 11 GeV Beam and a Polarized 3He Target in Hall C." Jefferson Lab Experiment E12-06-110, 2006 (with 2010 Update).

[14] B. Sawatzky (contact), T. Averett, W. Korsch, Z.-E. Meziani et al., "A Path to 'Color Polarizabilities' in the Neutron: A Precision Measurement of the Neutron g_2 and d_2 at High Q^2 in Hall C." Jefferson Lab Experiment E12-06-122, 2006 (with 2010 Update).

[15] M. L. Cardona, *Measuring the Neutron Spin Asymmetry A_1^n in the Valence Quark Region in Hall C at Jefferson Lab*, Ph.D. thesis, Temple U., Philadelphia, PA (United States), 2023. https://doi.org/10.34944/dspace/8548.

[16] M. Chen, *Precision Measurement of the Neutron Asymmetry A_1^n at Large Bjorken x at 12 GeV Jefferson Lab*, Ph.D. thesis, Physics - Graduate School of Arts and Sciences, University of Virginia, 2023. 10.18130/z76a-dz43.

[17] X. Zheng, *Precision Measurement of Neutron Spin Asymmetry A_1^n at Large xbj Using CEBAF at 5.7 GeV*, Ph.D. thesis, Massachusetts Inst. of Technology (MIT), Cambridge, MA (United States), 2002. https://www.osti.gov/biblio/824895.

[18] JEFFERSON LAB HALL A collaboration, D. Flay et al., *Measurements of d_2^n and A_1^n: Probing the neutron spin structure*, *Phys. Rev. D* **94** (2016) 052003, [1603.03612].

[19] S. Kuhn (contact), A. Deur, T. Forest, K. Griffioen, H. M., D. Keller et al., "Longitudinal Spin Structure of the Nucleon." Jefferson Lab Experiment E12-06-109, 2006 (with 2010 Update).

[20] C. Cotton, J. Smith and X. Zheng, "Exploring Quark Helicity Distributions with a 22 GeV Beam at Jefferson Lab." this proceedings, 2024.